CRATERING AND PENETRATION EXPERIMENTS IN ALUMINUM 1100 TARGETS USING SODA-LIME GLASS PROJECTILES FROM 1-7 KM/S

F. Hörz[①], M.J. Cintala[①], R.P. Bernhard[②] and T.H. See[②], [①]NASA - Johnson Space Center, Houston, Texas, 77058; [②]Lockheed - ESC, Houston, Texas 77058

INTRODUCTION: Using Teflon targets to simulate thermal blankets from the Long Duration Exposure Facility (LDEF), we demonstrated that it is possible to obtain unique solutions of projectile diameter (D_p) from diameter measurements of individual penetration holes (D_h) [1 & 2]. This renders the interpretation of penetration holes totally akin to that of craters in infinite halfspace targets. This new approach seems to be a substantial improvement over traditional ballistic-limit considerations [3 & 4], which typically yield a single, cumulative count for all projectiles larger than some threshold impactor capable of physically perforating a target of a given thickness (T).

The present work reports on equivalent *calibration*-type experiments with aluminum 1100 targets. Interest in this soft and relatively pure (>99% Al) alloy relates to surfaces that display sizable populations of craters and penetration holes on space-exposure surfaces from the Solar Maximum Mission (SMM; [4]) and LDEF [5, 6 & 7]. Furthermore, thin-films of pure aluminum are contemplated for use in future cosmic-dust instruments, either as the plasma-producing membranes in some trajectory sensor concepts, or in capture cells [8]. Lastly, past interpretations of SMM and LDEF features close to the ballistic limit tended to systematically yield larger impactors from penetration equations compared to cratering equations [4, 5, 7 & 9]. Therefore, it seemed appropriate to experimentally delineate, in detail, the transition from cratering to penetration processes in aluminum targets to resolve these apparent discrepancies, as we did for Teflon in our earlier experiments [1 & 2].

EXPERIMENTS: The experiments employed 3.2 mm (1/8") soda-lime glass projectiles and annealed aluminum 1100 targets; the thickness of the targets were systematically varied over approximately four orders of magnitude ($0.1 < D_p/T > 1000$) at any specific experimental velocity (2.0, 4.0, 5.0, 5. 9 and 6.7 km/s). Our database consists of ~35 cratering experiments [10] and 70 penetration events [11]. Crater diameter (D_c) was measured at the initial target surface; penetration-hole size (D_h) reflects the minimum diameter of the physical perforation, which can reside anywhere from close to the target's rear to close to the target's front side, depending on T.

RESULTS: Figure 1 illustrates the basic, dimensional measurements made for each of the experimental velocities. Open symbols refer to D_c measurements, closed symbols to D_h. In this portrayal, the "standard" craters in infinite halfspace targets form a horizontal (dashed) line, because D_c/D_p is a constant (the actual ratios are given in parenthesis in Figure 1). The very first perforations are "marginal" penetrations of $D_h < D_p$ (not illustrated due to space limitations), which substantially drive the steepening of the (solid) D_h curves. These D_h lines intercept the D_p/T axis at the exact ballistic-limit thickness (T_{BL}), where $D_h = 0$, by definition. This asymptotic approach to $D_h = 0$ results in a vertical line which separates cratering in infinite halfspace targets (stippled gray) from physical perforation. Obviously, increasingly higher velocities entail decreasing D_p/T values for T_{BL} (value in parenthesis). Marginally penetrated targets are characterized by crater rims and lips that are essentially indistinguishable from those of the standard crater. Indeed, the feature diameter at the target front side (D_c') is that of the standard crater (*i.e.*, $D_c' = D_c$), even for sizable penetration holes up to approximately $D_p/T = 1$. Most penetrations in such massive targets may be characterized by a D_c' and D_h measurement, yet the D_c' measurement is the more diagnostic. The arrows in Figure 1, at $D_p/T \sim 1$, illustrate the condition where the shock-pulse duration (t) in the projectile (t_p) and target (t_t) is exactly equal; these conditions were calculated following [12], using appropriate equation-of-state data [13]. We postulate that any condition of $t_p < t_t$ will produce material motions at and near the target surface that correspond to those of a full-fledged crater of diameter D_c. At $t_p > t_t$, these motions will be terminated at earlier times and (lateral) flow will be less than that of a standard crater, thus $D_h = D_c' < D_c$. As a consequence, the condition of $t_p = t_t$ characterizes the transition from cratering to penetration for the purpose of extracting projectile

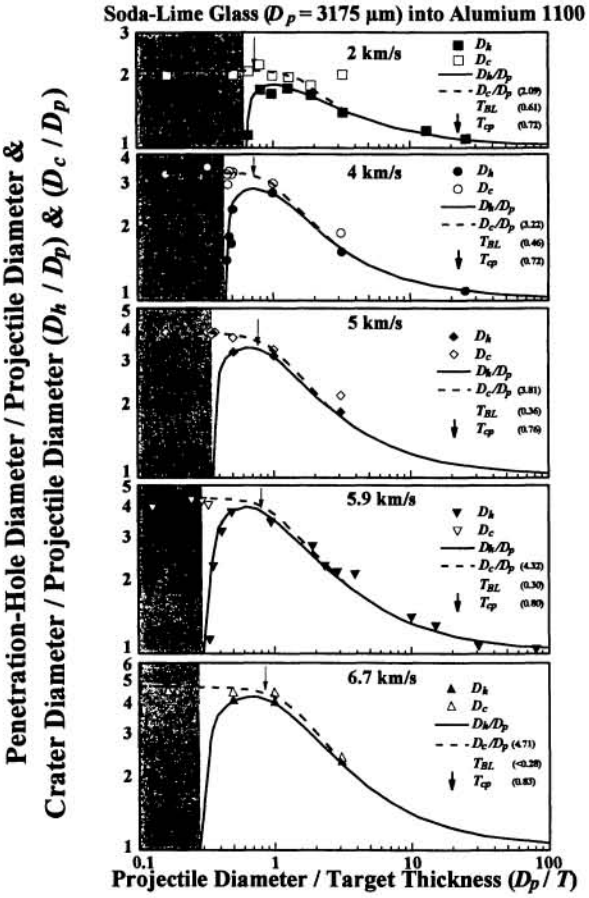

Figure 1. Crater (D_c) and penetration (D_h) diameters at each of the five experimental velocities.

dimensions from unknown penetrations. This transition is marked by an arrow in Figure 1 (T_{cp}) with the associated D_p/T values given in parenthesis. For $t_t << t_p$, the flow fields terminate at progressively shorter times to yield increasingly smaller holes until the condition of $D_h = D_p$ is reached. This typically occurs at $D_p/T \sim 100$, regardless of impactor velocity.

Figure 2 summarizes the same data in a somewhat simplified form by using only the larger of either D_c or D_h (solid lines), which we consider the primary measurements and criteria for the interpretation of space-produced penetrations. In addition, our suggestions for extrapolating the experimental observations to higher velocities are also portrayed (dashed lines). Based on the works of [3 & 9] one may calculate a standard crater diameter (D_c/D_p) at any velocity. This constant forms a horizontal line that ultimately intercepts the T_{cp} line, the latter being the locus of $t_t = t_p$ at any given velocity. All impacts to the left of this line should be interpreted as craters of diameter D_c, all events to the right as genuine penetrations of $D_c' < D_c$. Because all experiments in very thin targets resulted in $D_h = D_p$ at $D_p/T \sim 100$, regardless of projectile velocity, we assumed that even higher velocities will approximately comply with this constraint as well. It then simply becomes a matter of graphical extrapolation, approximating the experimental curves and trends as best as possible, to connect the $t_t = t_p$ point on the T_{cp} line with that of $D_h = D_p$ at $D_p/T = 100$. Each individual curve has a characteristic shape and specific slope at any given D_p/T, implying variable exponents of velocity for any given target thickness at constant encounter velocity. As a group the curves steepen with increasing velocity, because D_c/D_p increases with $V^{2/3}$ [3 & 9], whereas the condition of $D_h = D_p$ is (essentially) invariant with velocity, based on our new observations.

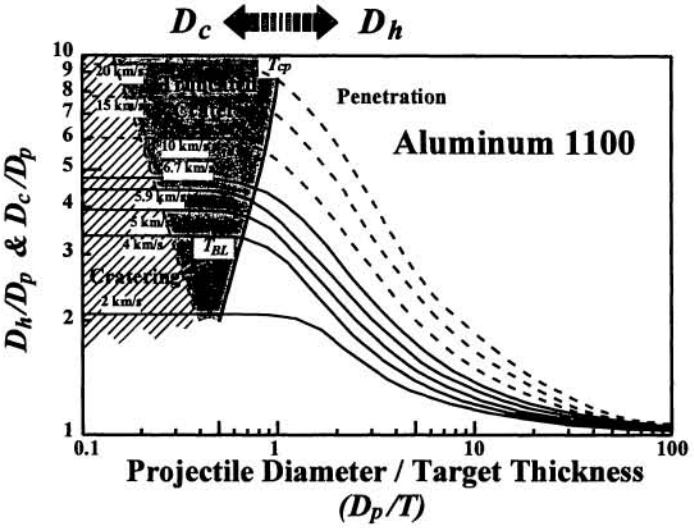

Figure 2. Summary plot of data portrayed in Figure 1. The solid lines represent a combination of the D_h curve and D_c line of Figure 1; dashed lines are extrapolations of the experimental data to higher velocities typical for LEO collisions.

The data illustrated in Figure 2 are replotted into Figure 3 to obtain unique *calibration curves* for D_p, at any assumed velocity, from a known target thickness (T) and measured hole diameter (D_h) on space-exposed surfaces. The horizontal termination of these curves at massive targets corresponds to the vertical line in Figure 2 and is driven by the condition of $D_h = 0$ at the ballistic limit.

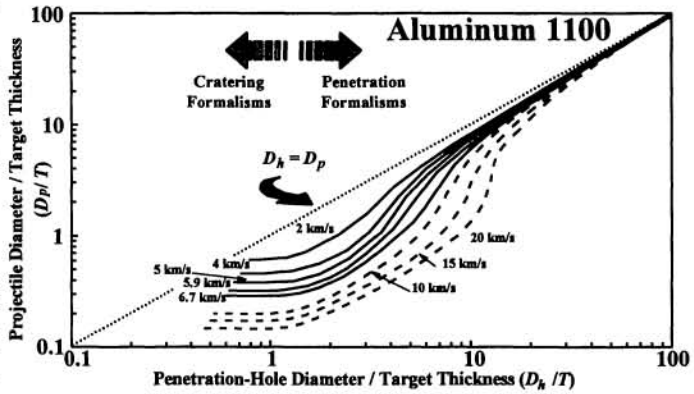

Figure 3. Calibration curves for D_p in aluminum 1100 targets.

CONCLUSIONS: These experiments demonstrate that unique solutions for D_p may be obtained from the diameter measurement of individual penetration holes in space-exposed aluminum 1100 targets, analogous to individual hypervelocity craters in infinite halfspace targets. However, there is no independent criteria from which to extract velocity information from the morphology of penetration holes, and it remains necessary to invoke reasonable estimates of encounter velocity. Finally, experimental work on the effects of projectile density and shape is needed to further aid in the interpretation of space-produced penetration holes.

REFERENCES: [1] Hörz *et al.* (1994), *LPSC XXV* (abstracts), 567-568; [2] Hörz *et al.* (1994), *NASA TM 104797*, 317 p.; [3] Cour-Palais, B.G. (1987), *Int. J. Impact Eng. 5*, 225-237; [4] McDonnell, J.A.M. and Sullivan, K (1992), in *Hypervelocity Impacts in Space*, Univ. of Kent, Canterbury; [5] Warren *et al.* (1989), *Proc. LPSC 19th*, 641-657; [6] See, T.H. *et al.* (1990), *NASA JSC Report # 24608*, 561p.; 7) Humes, D. (1992), *LDEF - 1st Post-Ret. Sym. NASA CP-3134*, 399-419; [8] Zolensky, M.E. (1994), *LPI Technical Report 94-05*, 101p.; [9] Watts *et al.*, *NASA Contractor Report 188259*, 102 p.; [10] Bernhard, R.P. and Hörz F. (1995), *Int. J. Impact Eng., HVIS 1994 Sym.*, in press; [11] Hörz *et al.* (1995), *NASA Tech. Memorandum*, in preparation; [12] Cintala, M.J. (1992), *J. Geophys. Res. 97*, 947-973; [13] Marsh, S.P. (1980), *LASL Hugoniot Data*, Univ. California Press.